WORLD CONFERENCE ON TIMBER ENGINEERING 2025
BRISBANE, AUSTRALIA
Advancing Timber for the Future Built Environment

ANALYTICAL APPROACH ON MOMENT PERFORMANCE OF GLUED-IN ROD TIMBER CONNECTION

Min-Jeong Kim[1], Jaewon Oh [2], Gwang Ryul Lee[3], Hae Seon Hwang[4], Chul-ki Kim[5], Jung-Kwon Oh[6]

ABSTRACT: This study evaluated the moment performance of beam-column timber connections using glued-in rods (GiR) and assessed the applicability of the theoretical model previously developed. In this study, we used a steel box to use different connection types for the beam and column joints of the beam-column connection. The beam connection utilized GiR connection integrated with a Slotted-in Plate (SIP), designed to distinctly allocate and resist shear force and moment. In this system, GiRs resist moment forces, while the SIP resists shear forces. In contrast, column connection employed a conventional GiR connection without SIP. This difference in connection type within beam-column connection was resulted from the distinct load distribution, as beams typically bear relatively greater shear force than columns. Both connection types exhibited ductile behavior with tensile failure of steel rods. The theoretical model showed reasonable agreement with experimental results for beam connection, particularly in rotational stiffness (-7.51% difference) and ultimate moment capacity (-3.27% difference). However, for the column connection where GiRs simultaneously resist both shear force and moment, the model showed considerable discrepancies. The results demonstrated that the theoretical model accurately predicted the behavior of the GiR connections with separated force mechanisms, while further research may be necessary for the conventional GiR connection.

KEYWORDS: *glued-laminated timber, Glued-in Rod (GiR), timber moment connection, beam-column connection*

1 – INTRODUCTION

The building and construction sector accounts for approximately 37% of global carbon dioxide emissions in 2022 [1], representing a significant contributor to climate change. In response to carbon reduction initiatives, including the Paris Agreement, there has been a growing emphasis on achieving carbon neutrality in the construction industry. This environmental imperative has led to increased interest in timber construction, which offers substantial environmental benefits and sustainable characteristics. Furthermore, the demand for mid- or high-rise timber structures increases.

The growing demand for massive timber structures has increased the need for reliable and efficient connection systems. This is because the overall structural capacity of the structures is largely determined by the strength and stiffness of these connections [2-6]. Among various connections, Glued-in Rod (GiR) connections have emerged as a promising solution. These connections consist of steel rods embedded in timber elements using structural adhesives. GiR connections offer higher load-bearing capacity and superior stiffness over traditional fastening methods. These connections can be concealed within timber elements, providing excellent fire resistance while preserving the natural aesthetics of timber structures [7]. Moreover, their simple configuration facilitates straightforward on-site assembly and simplifies the construction process [8,9]. The versatility of GIR connections allows implementation in various structural applications, ranging from simple beam-to-column joints to complex moment-resisting connections.

Given these advantages, there are various research has been continuously conducted to develop different types of connections utilizing GiR. Wakashima et al. [10] developed a semi-rigid connection system incorporating both lag screw bolts (LSB) and GiR. Additionally, Yang et al. [11] implemented a beam-column connection with GiR utilizing a steel box section. Furthermore, Stamatopoulos et al. [12] developed a connection with high stiffness by utilizing inclined GiRs. Recently, Oh et al. [13] developed a GiR connection system that employed a Slotted-in Plate (SIP) connection to separate shear force and moment. This system adopted a special force resistance mechanism, with the GiR specifically designed to resist only moment through a slotted hole while the SIP connection was dedicated to resisting shear force, thus improving the structural performance of the connection.

[1] Min-Jeong Kim, Dept. Agriculture, Forestry and Bioresources, Seoul National University, South Korea, minjeong.kim@snu.ac.kr
[2] Jaewon Oh, Department of Wood Science, University of British Columbia, Vancouver, Canada, jwoh@student.ubc.ca
[3] Gwang Ryul Lee, Dept. Agriculture, Forestry and Bioresources, Seoul National University, South Korea, qweqweqwer@snu.ac.kr
[4] Hae Seon Hwang, Dept. Agriculture, Forestry and Bioresources, Seoul National University, South Korea, haeseon@snu.ac.kr
[5] Chul-ki Kim, Wood Engineering Division, National Institute of Forest Science, Seoul, Republic of Korea, ckkim0407@korea.kr
[6] Jung-Kwon Oh, Dept. Agriculture, Forestry and Bioresources, Seoul National University, South Korea, jungoh@snu.ac.kr

https://doi.org/10.52202/080513-0622

Additionaly, there are analytical studies to develop the theoretical model to predict performance of GiR moment connections. Jensen and Quenneville [14] presented the ultimate resistance performance of GiR connections when subjected to either moment only or shear only. Navaratnam et al. [8] developed equations to predict moment resistance of GiR connection based on the pull-out performance of a single GiR rod connection. Oh et al. [13] also proposed equations to predict crucial parameters of GiR connection such as ultimate moment, initial rotational stiffness, and yield moment. Their model is also dependent on withdrawal capacity of rods.

Despite these advances in GiR connection research and analytical modeling, there remains a need to develop practical post-and-beam structural systems that utilize these GiR connections. Therefore, this whole research program aims to develop post-and-beam structures utilizing GiR beam-column connections. This study evaluates both the moment performance of the beam-column connections and the applicability of previously developed theoretical model to the connections.

2 – BACKGROUND

In this study, we utilized the GiR connection [13] for beam-column connection. This study was intended to develop a post-and-beam structure with an 8,000 mm span and 3,600 mm height. The timber members consisted of columns with dimensions of 210×420 mm and beams with dimensions of 210×600 mm (Fig. 1). Fragiacomo and Batchelar [7] reported that rods of GiR are inserted perpendicular to the grain direction, their moment capacity is reduced. Therefore, this study used a steel box to ensure that rods are inserted only parallel to the grain direction in beam-column connections. For clarity, the joint in the beam designated as the beam connection, while the joint in the column designated as the column connection. For the beam connection, the GiR moment connection with SIP [13] was adopted, and for the column connection, conventional GiR moment connection without SIP was adopted (Fig. 2). This differentiation in connection type was necessitated by the relatively higher shear force acting on beams compared to columns.

This study extended the work of the previous research by Oh et al. [13], where the performance evaluation of beam connections had been thoroughly completed. In this follow-up investigation, we applied identical testing methodologies to evaluate column connections, creating a comprehensive assessment framework for the entire post-and-beam structure. It is important to note that the beam connection results presented in this study are identical to those reported by [13].

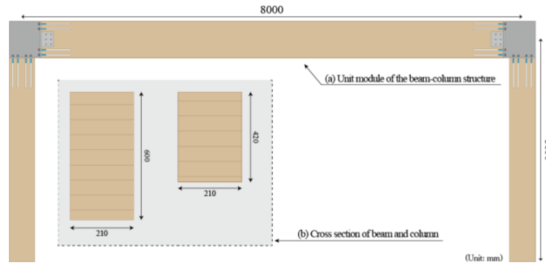

Figure 1. Geometry of The Beam-Column Structure in This Study

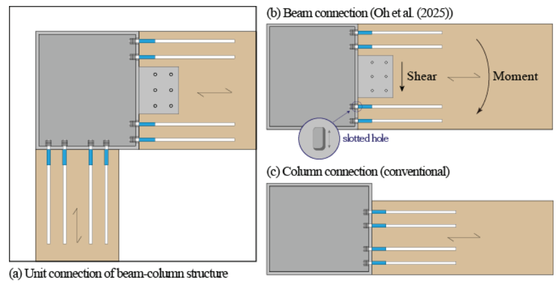

Figure 2. Connection Details of The Beam-Column Connection

3 – EXPERIMENTAL PROGRAM

3.1 SPECIMEN CONFIGURATIONS

The specimens were designed with the dimensions corresponding to the target timber members of the post-and-beam structure: beam connection (600×210 mm, already conducted) and column connection (420×210 mm). The differences between beam and column connection included not only the existence of SIP and member size, but also the rod hole configuration in H-beam and the end distance of rods. In the H-beam, beam connection utilized slotted holes (18×40 mm) to prevent shear resistance by vertical load, while column connection employed circular holes (Ø18 mm) to securely grip the rods. The end distance of beam connection was 40 mm (2.5d), while the end distance of column connection was 64 mm (4d). However, the rod spacing was maintained at 80 mm for both types. The end distance and rod spacing were based on the design recommendations from ETA [15].

All other configurations remained identical between beam and column connections. To examine the moment capacity of the connections, the specimens consisted of 2 m long Glued-laminated Timber (GLT) members connected perpendicularly to H-beams (H 400×400×13×21) with a length of 1.5 m. The H-beams were fixed to the ground through their flanges using twenty Ø22 mm bolts. The GiR connections contained eight threaded rods, each with a diameter of 16 mm, an anchorage length of 480 mm, and a nonbonded length of 80 mm. These rod specifications were determined based on prior research [16].

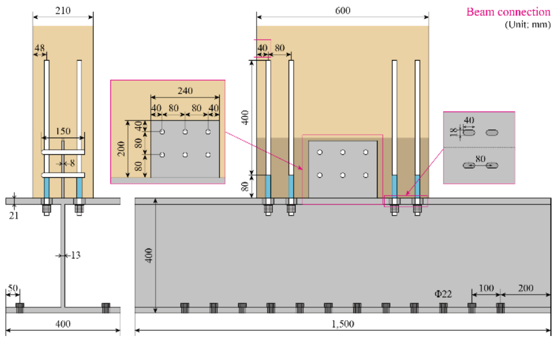

Figure 3. Configuration of Beam Connection [13]

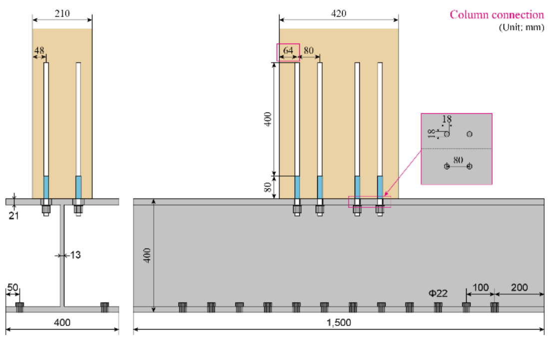

Figure 4. Configuration of Column Connection

3.2 MATERIALS

The timber members were manufactured using Japanese Larch(*Larix kaempferi*) as 10S-30B grade symmetrical GLT, as specified in KS F 3021 [17]. The average air-dry density of the larch GLT used in this test was measured as 492.7 kg/m³. The allowable tensile strength parallel to grain and modulus of elasticity are specified as 6.5 MPa and 8,000 MPa, respectively, according to KS F 3021. For the rod bonding, a two-component epoxy adhesive (HIT-RE 500 V3) was used. According to the manufacturer, the adhesive had an elastic modulus of 2,600 MPa and a bond strength of 11.7 MPa after 14 days of curing. The inserted rods were SS275 grade threaded rods conforming to KS D 3503 [18], with a yield strength of 275 MPa and a tensile strength of 410 MPa.

3.3 LOADING PROTOCOL

The moment capacity of the connections was evaluated using an actuator with ±225 kN maximum capacity and ±210 mm maximum displacement. Cyclic loading followed Method C (CUREE) as specified in ASTM E2126 [19]. While this standard typically recommends determining reference deformation through monotonic tests, it also allows for the use of reliable existing test data as an alternative. For the beam connection, Oh et al. [13] conducted one monotonic test and three cyclic tests. Therefore, in this follow-up study, we performed two cyclic tests only for the column connection based on the previous test results. The reference deformation was determined approximately 50 mm.

Figure 5. Photograph of Test for Column Connection

3.4 MEASUREMENT OF DISPLACEMENT AND ROTATION

For displacement measurements, Linear Voltage Displacement Transducers (LVDTs) were employed. The displacement measurement methodologies differed significantly between the beam connection and column connection, with substantial improvements implemented in the column connection to enhance measurement reliability. The beam connection test utilized only three LVDTs for measuring timber displacement and two LVDTs for H-beam displacement, whereas the column connection test employed a total of ten LVDTs, with five attached to the front face and five to the back face of the GLT, positioned at the all four rod locations and one at the center. Additionally, in the beam connection tests, the relative rotations were determined indirectly by measuring the GLT's rotation and the H-beam's rotation separately and then calculating the difference, whereas in the column connection tests, the relative displacement between the GLT and H-beam was measured directly. This method allows to enhance the reliability of the test results.

The displacements at each measurement point were determined by averaging the LVDT readings from both front and back faces of the GLT member. Local rotation angles between adjacent LVDT pairs were calculated using the arctangent of the difference between the sequential LVDT displacements divided by the specific distance between LVDTs (80 mm for LVDT1-2 and LVDT4-5; 66 mm for LVDT2-3 and LVDT3-4). The overall connection rotation was subsequently derived as the mean value of all calculated local rotation angles, providing a comprehensive representation of the rotational behavior across the entire connection interface.

https://doi.org/10.52202/080513-0622

$$\Delta_{LVDT,i} = \frac{\Delta_{LVDT,i,front} + \Delta_{LVDT,i,back}}{2} \quad (4)$$

$$\theta = mean\left[\sum_{i=1}^{4} \tan^{-1}\left(\frac{\Delta_{LVDT,i} - \Delta_{LVDT,i+1}}{\varphi}\right)\right] \quad (5)$$

Where,
h : height of timber member, mm
$\Delta_{LVDT,i}$:displacement measured by i-th LVDT, mm
φ : specific distance between LVDTs, mm

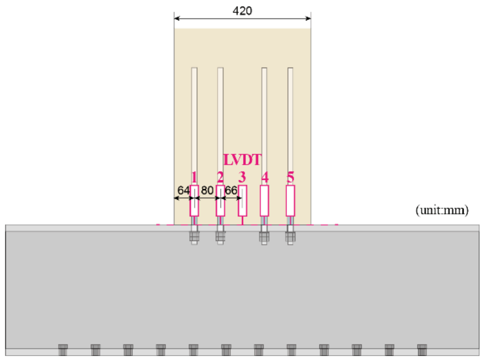

Figure 6. Arrangement of LVDTs for Column Connection

3.5 ANALYSIS METHOD OF TEST DATA

The moment was calculated by multiplying the test force by the moment arm length (1,850 mm). Initial rotational stiffness, yield and ultimate moment capacity were determined using hysterisis loop of cyclic test according to guideline by EN12512 [20]. The initial rotational stiffness was defined as the slope $(\tan\alpha)$ of the linear regression line through the moment-rotation data points between $0.1M_{max}$ and $0.4M_{max}$, where M_{max} was the maximum recorded moment. The ultimate moment strength (M_u) was defined as the point at which failure occurred or $0.8M_{max}$. The yield point was determined where the initial stiffness line intersects with a tangent line having a slope of 1/6 of the initial stiffness ($\tan\beta$ = 1/6 $\tan\alpha$), resulting in the yield moment (M_y) and yield rotation (θ_y). Ductility(μ) was determined by dividing the ultimate rotation by the yield rotation.

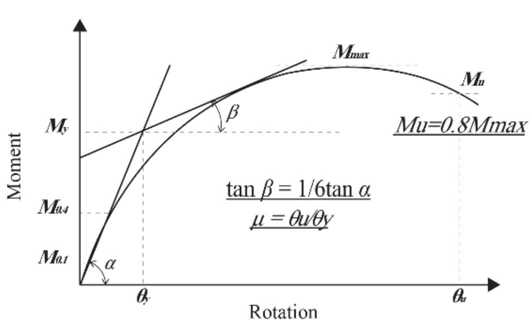

Figure 5. Definition of Yield and Ultimate Capacity of Timber Connection (EN 12512) [20]

4 – THEORETICAL MODEL

In this study, the theoretical model developed by Oh et al. [13] was adopted to predict the performance of the beam-column connections and to assess its applicability. The theoretical model for GiR connection was developed through the transformed section method by Fragiacomo and Batchelar [7], which serves as the analytical foundation. Additionally, the model conservatively assumed a bi-linear model for the GiR's rod behavior.

The theoretical model consists of three key formulas: initial rotational stiffness, yield moment capacity, and ultimate moment capacity. Both the initial rotational stiffness and yield moment capacity can be calculated by determining the neutral axis using fundamental principles of mechanics of materials—specifically, Hooke's law and force equilibrium within the linear elastic stage.

The ultimate moment capacity can be calculated under the assumption that the neutral axis shifts to the edge of the connection, with all rods reaching their yield strength.

1) The initial rotational stiffness

$$R = \frac{1}{10^6}\frac{M^*}{\theta} = K_{GIR}\sum_i\left[(d_i - a)\left(d_i - \frac{1}{3}a\right)\right] \quad (1)$$

Where,
a : distance from compression edge to neutral axis, mm
d_i: distance from compression edge to i-th rod, mm
K_{GIR} : withdrawal stiffness of glued-in rod, N/mm
M^*: applied bending moment at connection, N·mm
R : rotational stiffness of connection, kN·m/rad
θ : rotation angle of connection, rad

2) The yield moment capacity

$$M_y = \sum_i T_i\left(d_i - \frac{1}{3}a\right) = F_y\sum_i\frac{d_i - a}{d_{max} - a}\left(d_i - \frac{1}{3}a\right) \quad (2)$$

Where,
d_{max} : distance from compression edge to outermost rod, mm
T_i : tensile force of i-th glued-in rod, N

3) The ultimate moment capacity

$$M_u = \sum_i T_i d_i = F_y \sum_i d_i \quad (3)$$

In this study, we predicted the initial rotational stiffness, the yield moment capacity, and the ultimate moment capacity using these formulas, and compared these predictions with experimental values. Therefore, the applicability of the theoretical model to the connections was assessed.

https://doi.org/10.52202/080513-0622

5 – RESULTS AND DISCUSSIONS

5.1 PERFORMANCE OF THE CONNECTION

The experimental results from both connection types were presented in Table 1 and 2. Test specimens were designated using a three-part system: connection type (B: beam or C: column), loading protocol (M: Monotonic or C: Cyclic), and test sequence number. This naming system clearly identifies each specimen's configuration and testing conditions. For example, "B-M-1" indicates the first monotonic test on a beam connection.

The test results indicated that beam connections achieved an average maximum moment capacity of 259.41 kN·m, yield moment of 206.05 kN·m, and ultimate moment of 224.93 kN·m. The beam connections demonstrated an initial rotational stiffness of 47650.22 kN·m/rad. Meanwhile, column connections showed an average maximum moment of 115.87 kN·m, yield moment of 98.57 kN·m, and ultimate moment of 98.30 kN·m, with rotational stiffness of 15969.70 kN·m/rad.

Both beam and column connections exhibited identical failure behaviour. As loading progressed, the steel rods exhibited noticeable elongation, transitioning from elastic to plastic deformation illustrated in Fig. 7(a). The ultimate failure mode was characterized by the simultaneous breakage of all or some GIR rods positioned on the tension side illustrated in Fig. 7(b).

Fig. 8 presents the hysteresis loops and envelope curves for all specimens. The horizontal and vertical axes utilized different scales due to varying load magnitudes. These scale adjustments were made to ensure clear and accurate interpretation of the graphical data.

The cyclic loading tests revealed nearly symmetrical behavior between positive and negative envelope curves , with the exception of specimen C-C-2. Additionally, initial slips were observed in specimens B-C-1, B-C-2, and C-C-2, as shown in Fig. 8. This initial slip was considered to be a result of inconsistencies between the specimens in the manual tightening process when securing the rods of GiR to the H-beam flanges. The hand-tightening method likely produced non-uniform clamping forces, contributing to the observed initial slip behavior. Bouchard et al. [21] suggested that applying a consistent nut tightening method to achieve uniform torque helps minimize initial gaps in the GiR connection

(a) tensile yielding of steel rods (b) tensile failure of steel rods

Figure 7. Failure Mode of GiR Moment Connection

.

Table 1: Summary of Results from Connection Tests of Beam Connections

Specimen ID	M_{max}	θ_y	M_y	θ_u	M_u	μ	R
B-M-1	258.59	0.0078	223.50	0.0172	210.62	2.20	37301.11
B-C-1	258.16	0.0069	205.77	0.0194	236.66	2.83	40520.47
B-C-2	256.35	0.0059	206.69	0.0245	209.94	4.11	49209.62
B-C-3	264.55	0.0038	188.26	0.0205	242.48	5.41	63569.70
Average	259.41	0.0061	206.05	0.0204	224.93	3.64	47650.22
COV	1.37%	28.24%	6.98%	14.89%	7.59%	40.23%	24.22%

Table 2: Summary of Results from Connection Tests of Column Connections

Specimen ID	M_{max}	θ_y	M_y	θ_u	M_u	μ	R
C-C-1	116.75	0.0058	98.60	0.3060	93.84	5.29	17005.71
C-C-2	114.98	0.0095	98.00	0.0237	94.84	2.63	14933.70
Average	115.87	0.0076	98.30	0.0272	94.34	3.96	15969.70
COV	1.08%	34.15%	0.44%	17.85%	0.75%	47.47%	9.17%

R : the initial rotational stiffness (kN·m/rad)

M_{max},M_y, M_u : maximum/yield/ultimate moment capacity (kN·m)

θ_y, θ_u: yield/ultimate rotation angle (rad)

https://doi.org/10.52202/080513-0622

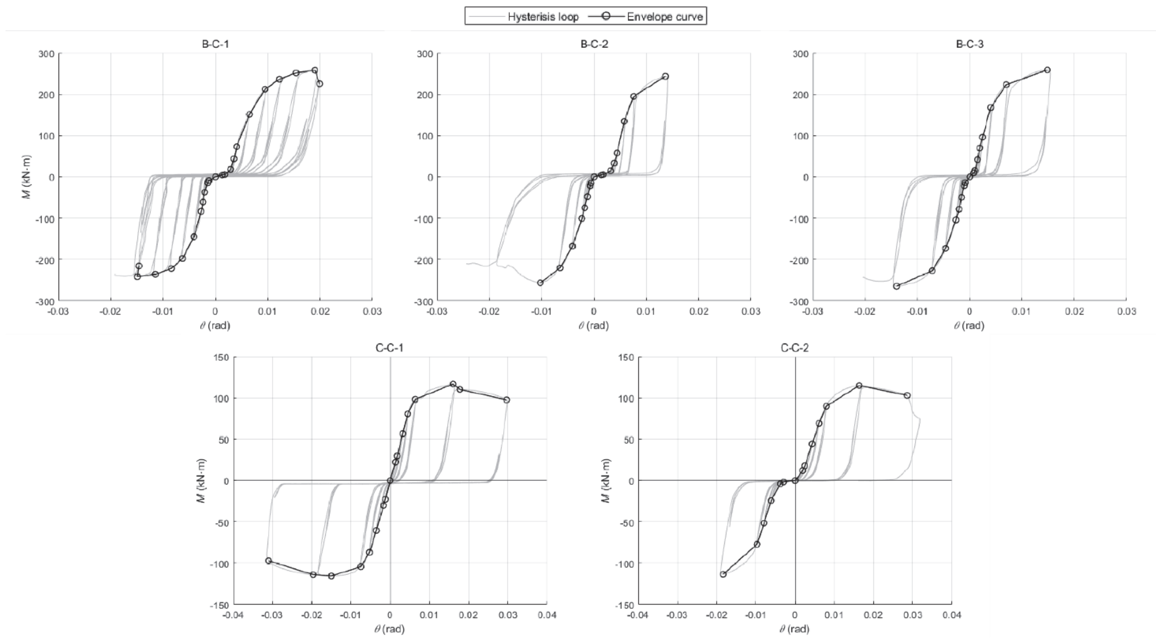

Figure 8. Hysterisis Loop and Envelop Curve of Beam and Colum Connections

5.2 ASSESSMENT OF THE MODEL

The average experimental results of both beam and column connections were compared with theoretical model predictions, and the results are summarized in Table 3. The theoretical model [13], which was used for the comparison, bases its formulas on the withdrawal capacity of rods. For our predictions, we calculated using the rod parameters such as K_{GIR} and F_y obtained from single rod GiR pull-out tests previously conducted [16]. Specifically, the values used were K_{GIR} of 89.11 kN/mm and F_y of 90.66 kN.

For beam connections, both the rotational stiffness and the ultimate moment capacity were predicted with high accuracy, showing differences of less than 8% (7.51% and 3.27%, respectively) as the model slightly underestimated these values. However, the model notably underestimated the yield moment by 31.54%. This discrepancy was primarily due to the yield point determination methodology specified in EN12512. These results validated that the theoretical model has high accuracy for GiR moment connections with SIP, with the exception of the yield moment predictions. Since this model is based on the withdrawal capacity of rods in GiR, it demonstrated good predictive performance in cases where the SIP connection allows the rods of GiR to resist moment exclusively without shear force. Furthermore, the accuracy of the predictions was achieved the fact that the connection failure mode was predominantly governed by rod failure.

In contrast, for column connections, some variations were observed between experimental results and theoretical model predictions. The model underestimated rotational stiffness by 12.50% and yield moment by 21.89%, while overestimating ultimate moment capacity by 61.45%. These observations indicated certain constraints in the direct application of the model to column connections. However, the model could still be conservatively applied for predicting the initial rotational stiffness. While yield moment predictions remained conservative for both connection types, the difference was less pronounced for column connections. This reduced discrepancy was likely resulted from the yield strength reduction caused by combined forces (shear and moment) acting on column connections.

The conservative prediction in the initial rotational stiffness of column connections possibly was resulted from the distinct deformation mechanisms at play. In column connections, the rods fitted relatively tightly in their holes, restricting movement and resulting in less deformation. Conversely, in beam connections, the presence of slotted holes presumably allows for greater rod deformation. This difference in rod's hole configuration conditions offered one plausible explanation for why column connections exhibited higher experimental stiffness than predicted by the theoretical model.

For ultimate moment capacity of column connection, the experimental values were significantly lower than theoretical model predictions. This substantial discrepancy originated from the fundamentally different post-yield behaviors observed in the moment-rotation curves. While beam connections maintained consistent strength levels after yielding, column connections exhibited a pronounced decrease in strength capacity through the plastic deformation range. This behavior suggested that in column connections, the combined action of moment and shear force led to strength reduction after yielding.

These results emphasized the importance of developing more comprehensive analytical approaches that account for the effects of combined forces on connection behavior. Further research is needed to better understand the interaction between moment and shear force in GiR connections, particularly in post-yield behavior region.

Table 3: Comparison of Connection Moment Capacity between Average Test Results and Model Predictions

Property	Beam connection			Column connection		
	R	M_y	M_u	R	M_y	M_u
Average Experimental Value	47650.22	206.05	224.93	15969.70	98.30	94.34
Model Prediction	44069.63	141.07	217.58	13973.97	76.78	152.31
Difference	-7.51%	-31.54%	-3.27%	-12.50%	-21.89%	61.45%

6 – CONCLUSIONS

This study served as a follow-up to the research conducted by Oh et al. [13] on the GiR moment connection development and analytical modeling. This study evaluated the moment performance of beam-column GiR connections and assessed the applicability of the theoretical model. Two different connection types were examined: the GiR connection with the SIP for beam connection, and the conventional GiR connection for the column connection. Both connections demonstrated ductile behavior with failure primarily occurring through tensile yielding of steel rods.

The theoretical model showed excellent agreement with experimental results for beam connections, particularly in rotational stiffness (7.51% difference) and ultimate moment capacity (-3.38% difference). This validated the model was appropriate to predict the performance of GiR connections with SIP. The close agreement confirmed that the SIP effectively separates moment and shear force in the rods of the connection, aligning with the model's theoretical foundation. Because the model was only based on the withdrawal capacity of rods.

However, some discrepancies were observed between the model predictions and experimental results for column connections, with differences of -12.50% in rotational stiffness, -21.89% in yield moment, and 61.45% in ultimate moment capacity. These substantial variations indicated that the current theoretical model has limitations when applied to rods in the GiR connections subjected to combined forces (moment and shear).

These findings emphasize the importance of developing more comprehensive analytical approaches that consider the influence of combined forces on connection behavior. This might be especially relevant for understanding post-yield strength deterioration in conventional GiR connections without force separation mechanisms. Further research is needed to refine the theoretical model for better prediction of GiR connection behavior under combined loading conditions.

7 – REFERENCES

[1] United Nations Environment Programme, 2023 Global Status Report for Buildings and Construction: Beyond foundations - Mainstreaming sustainable solutions to cut emissions from the buildings sector. United Nations Environment Programme, 2024. doi: 10.59117/20.500.11822/45095.

[2] E. Poletti, G. Vasconcelos, J. M. Branco, and A. M. Koukouviki, "Performance evaluation of traditional timber joints under cyclic loading and their influence on the seismic response of timber frame structures," Construction and Building Materials, vol. 127, pp. 321–334, Nov. 2016, doi: 10.1016/j.conbuildmat.2016.09.122.

[3] J. Cao, H. Xiong, and Y. Cui, "Seismic performance analysis of timber frames based on a calibrated simplified model," Journal of Building Engineering, vol. 46, p. 103701, Apr. 2022, doi: 10.1016/j.jobe.2021.103701.

https://doi.org/10.52202/080513-0622

[4] R. Tomasi, M. A. Parisi, and M. Piazza, "Ductile Design of Glued-Laminated Timber Beams," Pract. Period. Struct. Des. Constr., vol. 14, no. 3, pp. 113–122, Aug. 2009, doi: 10.1061/(ASCE)1084-0680(2009)14:3(113).

[5] N. Satheeskumar, D. J. Henderson, J. D. Ginger, and C. H. Wang, "Finite element modelling of the structural response of roof to wall framing connections in timber-framed houses," Engineering Structures, vol. 134, pp. 25–36, Mar. 2017, doi: 10.1016/j.engstruct.2016.12.034.

[6] H. Ren, A. Bahrami, M. Cehlin, and M. Wallhagen, "A state-of-the-art review on connection systems, rolling shear performance, and sustainability assessment of cross-laminated timber," Engineering Structures, vol. 317, p. 118552, Oct. 2024, doi: 10.1016/j.engstruct.2024.118552.

[7] M. Fragiacomo and M. Batchelar, "Timber Frame Moment Joints with Glued-In Steel Rods. I: Design," J. Struct. Eng., vol. 138, no. 6, pp. 789–801, Jun. 2012, doi: 10.1061/(ASCE)ST.1943-541X.0000419.

[8] S. Navaratnam, J. Thamboo, T. Ponnampalam, S. Venkatesan, and K. B. Chong, "Mechanical performance of glued-in rod glulam beam to column moment connection: An experimental study," Journal of Building Engineering, vol. 50, p. 104131, Jun. 2022, doi: 10.1016/j.jobe.2022.104131.

[9] G. Tlustochowicz, E. Serrano, and R. Steiger, "State-of-the-art review on timber connections with glued-in steel rods," Mater Struct, vol. 44, no. 5, pp. 997–1020, Jun. 2011, doi: 10.1617/s11527-010-9682-9.

[10] Y. Wakashima, K. Okura, and K. Kyotani, "DEVELOPMENT OF DUCTILE SEMI-RIGID JOINTS WITH LAGSCREWBOLTS AND GLUED-IN RODS," 2010. Accessed: Mar. 06, 2025. [Online]. Available: https://www.semanticscholar.org/paper/DEVELOPMENT-OF-DUCTILE-SEMI-RIGID-JOINTS-WITH-AND-Wakashima-Okura/d291c86661277e9edbc89e62e2e2258a91ac5326

[11] H. Yang, W. Liu, and X. Ren, "A component method for moment-resistant glulam beam–column connections with glued-in steel rods," Engineering Structures, vol. 115, pp. 42–54, May 2016, doi: 10.1016/j.engstruct.2016.02.024.

[12] H. Stamatopoulos, K. A. Malo, and A. Vilguts, "Moment-resisting beam-to-column timber connections with inclined threaded rods: Structural concept and analysis by use of the component method," Construction and Building Materials, vol. 322, p. 126481, Mar. 2022, doi: 10.1016/j.conbuildmat.2022.126481.

[13] J. Oh, K.-S. Ahn, G. R. Lee, M.-J. Kim, S.-H. You, and S.-J. Pang, "Design and Analysis of Timber Moment Connections with Decoupled Glued-in Rods and a Slotted-in Plate".

[14] J. L. Jensen and P. Quenneville, "CONNECTIONS WITH GLUED-IN RODS SUBJECTED TO COMBINED BENDING AND SHEAR ACTIONS".

[15] European Organisation for Technical Assessment (ETA), Design of Glued-in Rods for Tibmer Connections.

[16] J. Oh et al., "Theoretical modeling of pull-out stiffness of glued-in single rod in timber," Engineering Structures, vol. 325, p. 119346, Feb. 2025, doi: 10.1016/j.engstruct.2024.119346.

[17] KS F 3021: Structural Glued-Laminated Timber, 2022.

[18] KS D 3503: Structural Steel.

[19] E06 Committee, Test Methods for Cyclic (Reversed) Load Test for Shear Resistance of Vertical Elements of the Lateral Force Resisting Systems for Buildings. doi: 10.1520/E2126-11.

[20] C. EN, "12512; Timber Structures—Test Methods—Cyclic Testing of Joints Made with Mechanical Fasteners," European Committee for Standardization, Brussels, Belgium, 2001.

[21] R. Bouchard, A. Salenikovich, C. Frenette, and G. Bedard-Blanchet, "Experimental investigation of joints with multiple glued-in rods in glued-laminated timber under axial tensile loading," Construction and Building Materials, vol. 293, p. 122614, Jul. 2021, doi: 10.1016/j.conbuildmat.2021.122614.

ACKNOWLEDGEMENT

This study was conducted with the support of R&D Program for Forest Science Technology (Project No. 2023494B10-2325-AA02) provided by Korea Forest Service (Korea Forestry Promotion Institute).

DECLARATION OF GENERATIVE AI AND AI-ASSISTED TECHNOLOGIES IN THE WRITING PROCESS

During the preparation of this work the authors used Claude AI to improve the language and readability of the manuscript. After using this tool, the authors reviewed and edited the content as needed and take full responsibility for the content of the publication.

https://doi.org/10.52202/080513-0622